Electronic Supplementary Material (ESI) for ChemComm.
This journal is © The Royal Society of Chemistry 2020

Three colour solid-state luminescence from positional isomers of facilely to modify thiophosphoranyl anthracenes

Timo Schillmöller, Paul Niklas Ruth, Regine Herbst-Irmer, and Dietmar Stalke*

Supporting Information

Content:

S1. General Information

Reactions using air- and moisture sensitive compounds were performed under an atmosphere of N_2 or Ar using Standard Schlenk techniques.[1] Solvents were dried with Standard techniques. Commercially available 1-Chloroanthraquinone and 2-Aminoanthraquinone were purchased and used without further purification. Chlorodiphenylphosphine was distilled before use. Elemental Sulfur was purified by sublimation. UV/Vis and fluorescence measurements were performed in Analytical grade solvents. For the sample preparation of the solid samples several single crystals were picked from the flask and their unit cells were determined. For the measurement the crystals were slightly ground to obtain a homogenous microcrystalline sample, which was used for the measurements.

NMR spectroscopic data were recorded on a Bruker Avance 300 MHz spectrometer and referenced to the deuterated solvent ($CDCl_3$).

Mass spectrometry has been carried out by the Central Analytical Unit of the *Institute of Organic and Biomolecular Chemistry* at the *Georg-August-University*, Göttingen. EI spectra were recorded using a *MAT 95* device with electron ionization (EI-MS: 70 eV). ESI spectra were obtained from a BRUKER micrOTOF instrument.

Elemental analyses (C, H, S) were carried out on a Vario EL3 at the Mikroanalytisches Labor, Institut für Anorganische Chemie, University of Göttingen.

UV/Vis spectra were recorded on an Agilent Cary 50 spectrometer using quartz cuvettes.

Fluorescence measurements were carried out on a HORIBA Jobin-Yvon Fluoromax-4 spectrometer equipped with a 150 W xenon arc lamp as excitation source and a photomultiplier as detector. A front-face setup was used for collecting emission spectra of solid samples. Absolute quantum yields were determined with the Quanta-φ integrating sphere. Lifetime measurements were performed with the TCSPC setup using a pulsed laser diode at 375 nm as excitation source.

The overlaps of the anthracene planes were calculated via the following procedure: A mean plane is fitted through the carbon atoms of the first anthracene. The carbon atom positions of both anthracene moieties are projected onto this mean plane, yielding a two dimensional polygon each. An intersection polygon is determined from the two. Finally, the overlap is calculated as the ratio of the intersection polygon area and the area of the two dimensional polygon from the first anthracene.

The Crystallographic Information Files (CIF) can be obtained free of charge from the Cambridge Crystallographic Data Centre via www.ccdc.cam.ac.uk/structures/ using the reference numbers 1993261-1993262.

S2. Experimental Details

1-Chloroanthracene[2] and 2-Bromoanthracene[3] were prepared according to literature procedures.

Synthesis of [1-(S)$PPh_2(C_{14}H_9)$] (**1**)

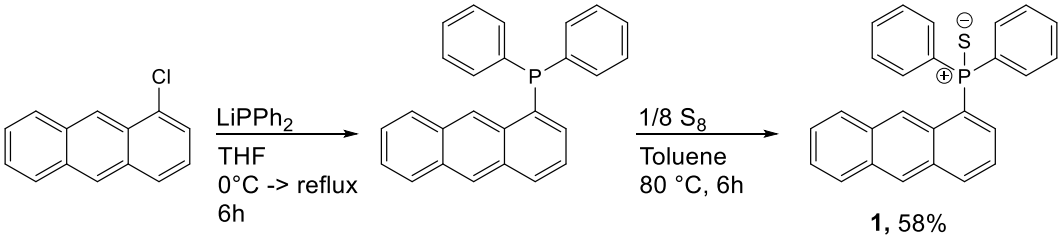

Scheme S1. Synthesis of [1-(S)$PPh_2(C_{14}H_9)$] (**1**).

To a solution of 1-chloroanthracene (0.48 g, 2.2 mmol, 1.0 eq.) in THF (10 mL) lithium diphenlyphosphanide in THF (0.5 M, 4.4 mL, 2.2 mmol, 1.0 eq) was added dropwise at 0 °C. After stirring for 10 min the red solution was allowed to reach room temperature and stirred for further 30 min. Afterwards the mixture was heated to reflux for 2 h. After cooling to ambient temperature, the reaction was quenched by adding of H_2O. Further H_2O was added until a precipitate formed. The solid was filtered off and washed with water and hexane. After drying under reduced pressure, the P(III) compound [1-$PPh_2(C_{14}H_9)$] was obtained. The oxidation was performed with elemental sulfur (0.106 g, 3.3 mmol, 1.5 eq.) in toluene (10 mL) over the course of 6 h at 80 °C. The precipitate was filtered off and re-crystallised from toluene to obtain **1** as a yellow solid.

Yield 0.503 g (58%). Yellow crystals. ^{1}H NMR (300 MHz, $CDCl_3$) δ [ppm] = 9.11 (s, 1 H, H_9), 8.47 (s, 1 H, H_{10}), 8.16 – 8.12 (m, 1 H, H_4), 7.98 – 7.94 (m, 1 H, H_5), 7.92 – 7.94 (m, 4 H, *o*-Ph), 7.80 – 7.76 (m, 1 H, H_8), 7.57 – 7.37 (m, 8 H, *p*-Ph, *m*-Ph, $H_{6,7}$) , 7.35 – 7.30 (m, 1 H, H_2), 7.28 – 7.18 (m, 1 H, H_3). ^{13}C{^{1}H} NMR (75 MHz, $CDCl_3$) δ [ppm] = 133.7 (d, ^3J(C,P) = 12.5 Hz, C_3), 133.7 (s, C_4), 132.5 (d, ^2J(C,P) = 10.7 Hz, *o*-Ph), 132.5 (d, ^1J(C,P) = 84.9 Hz, *i*-Ph), 132.1 (d, ^3J(C,P) = 8.6 Hz, C_{4a}), 131.6 (d, ^4J(C,P) = 3.2 Hz, *p*-Ph), 131.6 (s, C_{8a}), 131,5 (s, C_{10a}), 129.7 (d, ^1J(C,P) = 84.6 Hz, C_1), 129.2 (d, ^2J(C,P) = 9.07 Hz, C_{9a}), 129.0 (s, C_8), 128.7 (d, ^3J(C,P) =12.6 Hz, *m*-Ph, 127.8 (d, *J*(C,P) = 7.1 Hz, C_9), 127.6 (d, ^4J(C,P) = 1.3 Hz, C_{10}), 127.6 (s, C_5), 126.2 (s, C_7), 125.9 (s, C_6), 123.5 (d, ^2J(C,P) = 14.7 Hz, C_2). ^{31}P{^{1}H} NMR (121 MHz, $CDCl_3$) δ [ppm] = 42.10. HRMS (EI): calc. for $[C_{26}H_{19}PS]^+$: 394.0945, found: 394.0944. Elemental Analysis: calc: C: 79.17, H: 4.86, S: 8.13; found: C: 79.83, H: 4.73, S: 8.56.

Synthesis of [2-(S)$PPh_2(C_{14}H_9)$] (**2**)

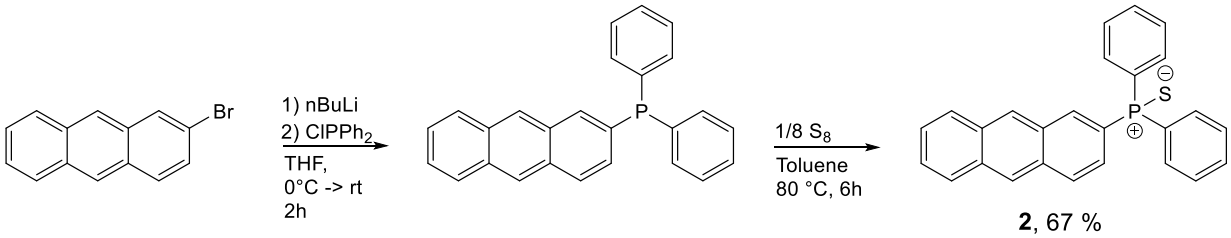

Scheme 2. Synthesis of [2-(S)$PPh_2(C_{14}H_9)$] (**2**).

2 was prepared similar to the previously reported [9-(S)$PPh_2(C_{14}H_9)$]: 2-bromoanthracene (0.40 g, 1.6 mmol, 1.0 eq.) was suspended in Et_2O (15 mL) and cooled to 0 °C. *n*Butyllithium in hexane (2.2 M, 0.11 g, 1.7 mmol, 1.1 eq.) was added slowly and the mixture stirred for 10 min and then allowed to reach ambient temperature. After the solid was completely dissolved the mixture was cooled to 0 °C again and chlorodiphenylphosphane (0.38 g, 0.31 mL, 2.4 mmol, 1.1 eq.) was added dropwise. The solution turned red and a precipitate formed immediately. The mixture was warmed to ambient temperature and stirred for another 2 h and the precipitate was filtered off. The precipitate was dissolved in toluene (10 mL) and filtered again for removal of LiCl. Removal of the solvent under reduced pressure afforded the phosphane [2-$PPh_2(C_{14}H_9)$]. Sulfur-oxidation was performed with elemental sulfur (0.077 g, 2.4 mmol, 1.5 eq.) in toluene (10 mL) at 80 °C for 6 h. After cooling to ambient temperature, the precipitate was filtered off and the target compound was obtained as a pale-yellow solid. Recrystallisation from toluene afforded single crystals suitable for X-ray structure determination.

Yield 0.423 g (67%). Yellow crystals. ^{1}H NMR (300 MHz, $CDCl_3$) δ [ppm] = 8.45 (s, 2H, $H_{9,10}$), 8.41 – 8.35 (m, 1H, H_1), 8.06 – 7.98 (m, 3H, $H_{3,5,8}$) 7.85 – 7.78 (m, 4H, *o*-Ph), 7.71 – 7.64 (m, 1H, H_4), 7.58 – 7.44 (m, 8H, *m*-Ph, *p*-Ph, $H_{6,7}$). ^{13}C{^{1}H} NMR (75 MHz, $CDCl_3$) δ [ppm] = 135.2 (d, ^2J(C,P) = 10.4 Hz, 1C, C_1), 133.2 (d, J(C,P) = 17.0 Hz, 1C, C_2), 132.4 (d, ^2J(C,P) = 10.7 Hz, 4C, *o*-Ph), 132.2 (s, 1C, C_{8a}), 131.7 (d, ^3J(C,P) = 2.3 Hz, 1C, C_{9a}), 131.6 (d, ^4J(C,P) = 2.0 Hz, 2C, *p*-Ph) 130.2 (s, 1C, C_{4a}), 130.0 (d, J(C,P) = 11.4 Hz, 2C, *i*-Ph), 128.8 (d, ^2J(C,P) = 19.8 Hz, 1C, C_3), 128.0 (s, 1C, C_{10a}), 128.6 (d, ^3J(C,P) = 12.6 Hz, 4C, *m*-Ph), 128.4 (s, 2C, $C_{5,8}$), 128.2 (d, ^4J(C,P) = 7.3 Hz, 1C, C_9), 126.3 (s, 1C, C_{10}), 126.3 (s, 2C, $C_{6,7}$), 125.6 (d, ^3J(C,P) = 11.4 Hz, 1C, C_4). ^{31}P{^{1}H} NMR (121 MHz, $CDCl_3$) δ [ppm] = 43.60. HRMS (ESI^+): calc. for $[C_{26}H_{20}PS]^+$: 395.1018, found: 395.1014. Elemental Analysis: calc: C: 79.17, H: 4.86, S: 8.13; found: C: 78.96, H: 4.71, S: 8.36.

S3. X-Ray Crystallographic Analysis

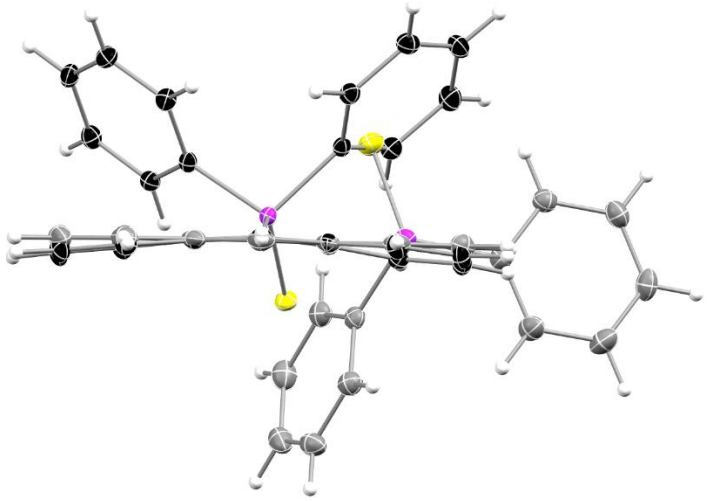

Fig. S1. Overlay of the solid-state structures of **1** (grey) and **3** (black) showing the pronounced folding of the anthracene in **3**.

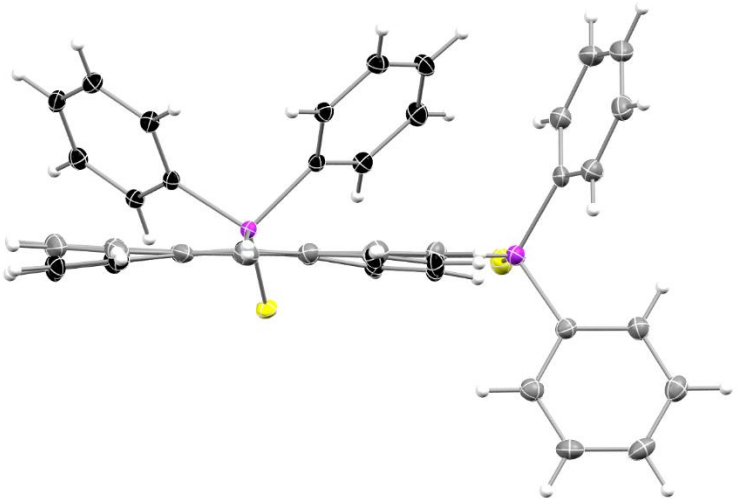

Fig. S2. Overlay of the solid-state structures of **2** (grey) and **3** (black) showing the pronounced folding of the anthracene in **3**.

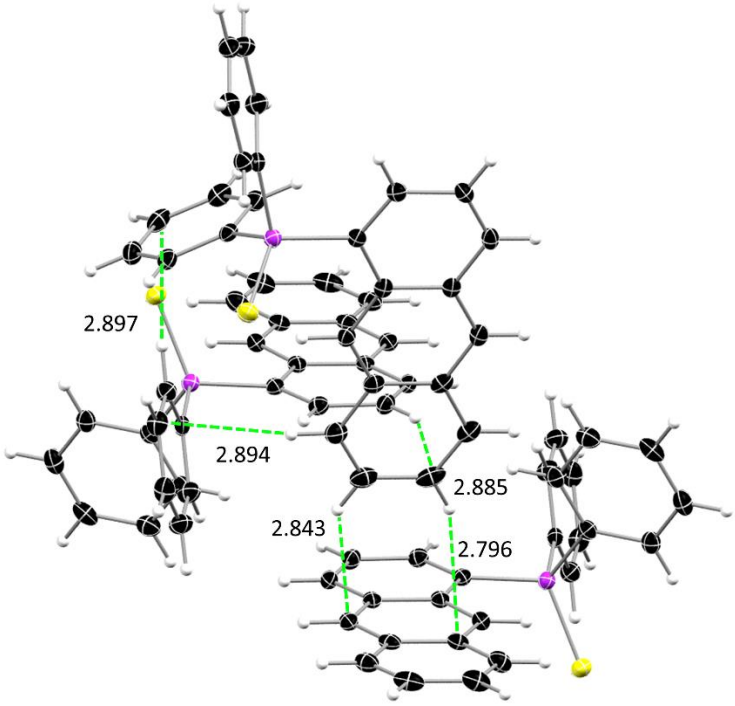

Fig. S3. Shortest C–H ··· π interactions (in Å) as found in the solid-state structure of **1.**

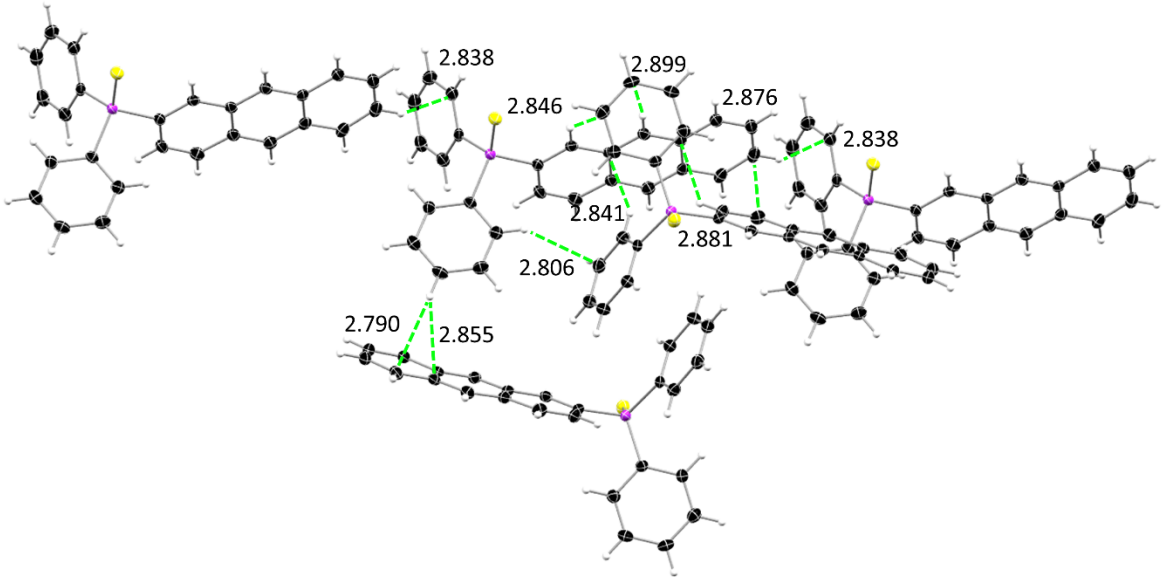

Fig. S4. Shortest C–H ··· π interactions (in Å) as found in the solid-state structure of **2.** Disorder is omitted for clarity.

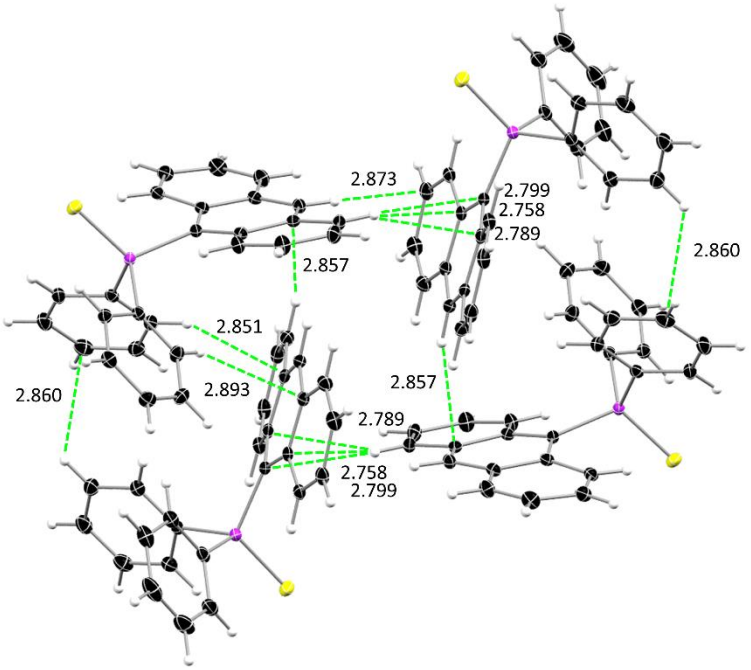

Fig. S5. Shortest C–H ··· π interactions (in Å) as found in the solid-state structure of **3.**

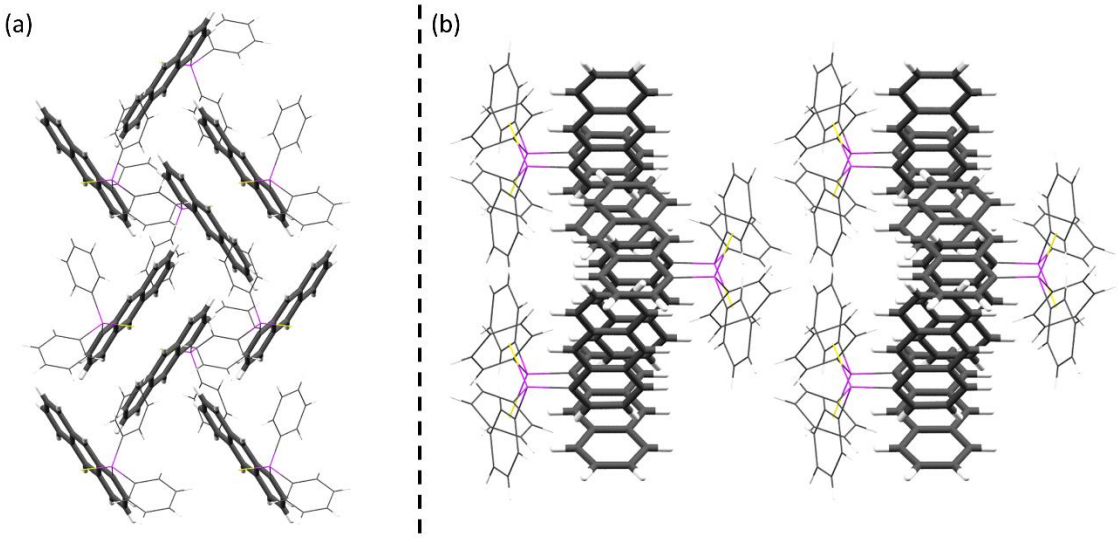

Fig. S6. (a) Crystal packing of **1** with view along the crystallographic a-axes and (b) along the crystallographic c-axes. The anthracene moieties are highlighted.

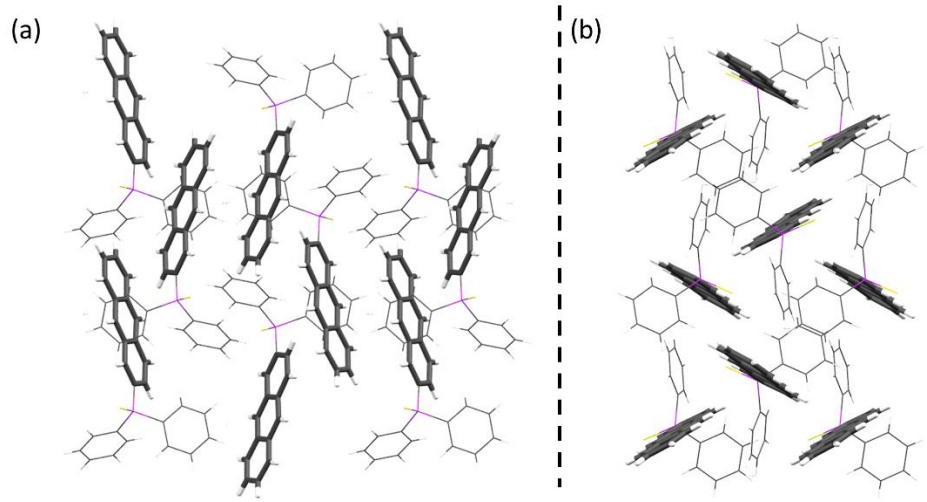

Fig. S7. (a) Crystal packing of **2** with view along the crystallographic a-axes and (b) along the crystallographic c-axes. The anthracene moieties are highlighted. Disorder is omitted for clarity.

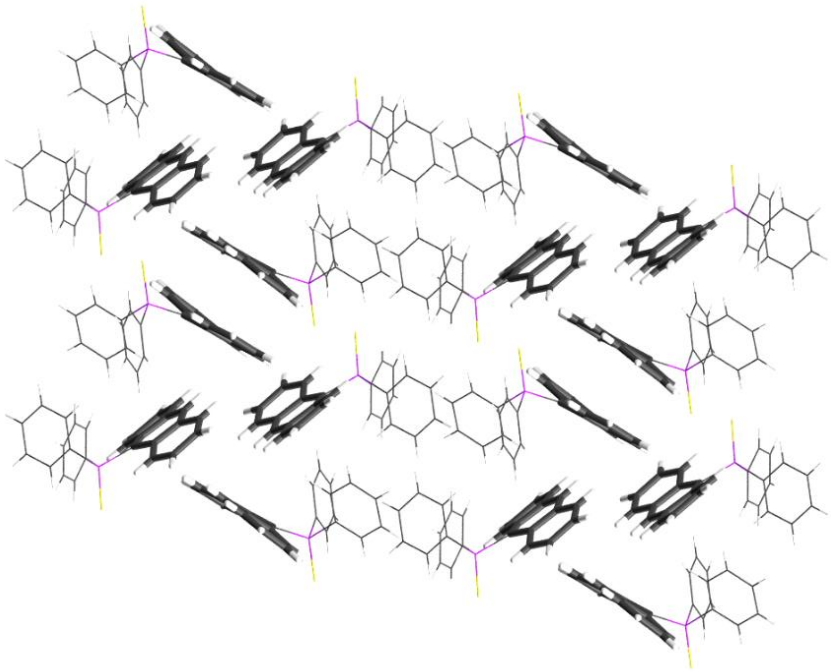

Fig. S8. Crystal packing of **3** with view along the crystallographic a-axes. The anthracene moieties are highlighted.

Table S1. Crystallographic data of thiophosphoranyl anthracenes **1** and **2.**		
	1	**2**
CCDC	1993261	1993262
Empirical formula	$C_{26}H_{19}PS$	$C_{26}H_{19}PS$
Formula weight [g/mol]	394.44	394.44
Temperature [K]	100(2)	100(2)
Wavelength [Å]	0.71073	0.71073
Crystal system	Monoclinic	Monoclinic
space group	$P2_1/c$	$P2_1/n$
a [Å]	13.967(2)	9.649(2)
b [Å]	8.892(2)	16.139(3)
c [Å]	17.201(3)	13.295(3)
β [°]	110.46(4)	109.43(2)
Volume [Å^3]	2001.5(8)	1952.5(7)
Z	4	4
ρ_{calc} [Mg/m^3]	1.309	1.342
μ [mm^{-1}]	0.250	0.257
F(000)	824	824
Crystal size [mm]	0.153 x 0.152 x 0.107	0.226 x 0.125 x 0.109
θ range [°]	1.556 to 26.440	2.057 to 26.743
Reflections collected	47172	40967
Independent reflections	4113	4151
R(int)	0.0628	0.0553
Max. / min. transmission	0.7454 / 0.7083	0.7454 / 0.7056
Restraints / parameter	0 / 253	695 / 344
GooF	1.034	1.110
R1 / *w*R2 (I > 2σ(I))	0.0340 / 0.0787	0.0453 / 0.0980
R1 / *w*R2 (all data)	0.0457 / 0.0855	0.0549 / 0.1019
max. diff peak / hole [e Å^{-3}]	0.345 / -0.319	0.370 / -0.400

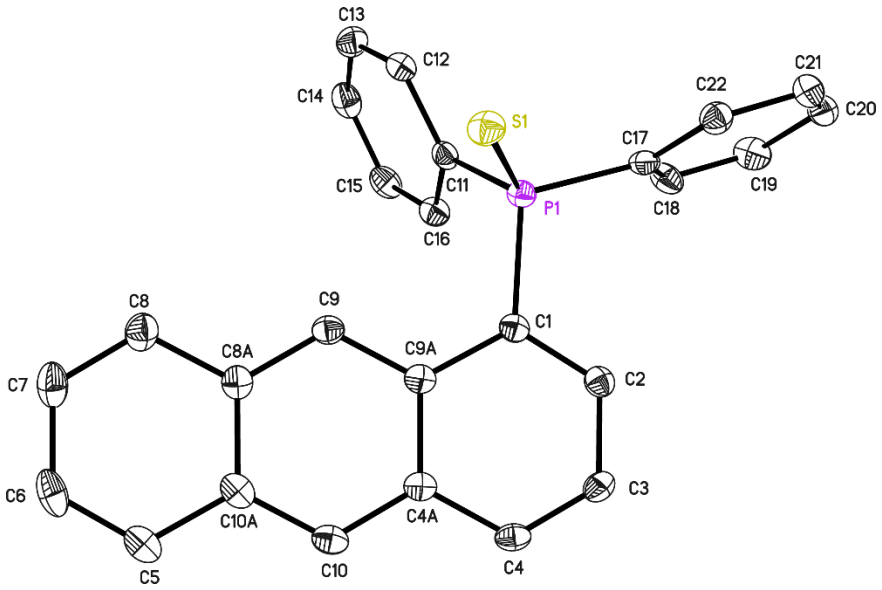

Fig. S9. Asymmetric unit of **1** with anisotropic displacement parameters at 50 % probability level. Hydrogen atoms are omitted for clarity.

Table S2. Bond lengths [Å] and angles [°] for **1**.			
P(1)-C(1)	1.8135(17)	C(11)-P(1)-C(17)	104.62(8)
P(1)-C(11)	1.8203(18)	C(1)-P(1)-S(1)	113.87(6)
P(1)-C(17)	1.8208(18)	C(11)-P(1)-S(1)	113.37(6)
P(1)-S(1)	1.9579(7)	C(17)-P(1)-S(1)	112.22(6)
C(1)-C(2)	1.371(2)	C(2)-C(1)-C(9A)	120.00(15)
C(1)-C(9A)	1.447(2)	C(2)-C(1)-P(1)	119.25(13)
C(9A)-C(9)	1.400(2)	C(9A)-C(1)-P(1)	120.57(12)
C(9A)-C(4A)	1.440(2)	C(9)-C(9A)-C(4A)	118.22(15)
C(2)-C(3)	1.420(2)	C(9)-C(9A)-C(1)	123.81(15)
C(3)-C(4)	1.353(2)	C(4A)-C(9A)-C(1)	117.96(15)
C(4)-C(4A)	1.430(2)	C(1)-C(2)-C(3)	121.49(16)
C(10A)-C(10)	1.396(2)	C(4)-C(3)-C(2)	120.01(16)
C(10A)-C(5)	1.428(2)	C(3)-C(4)-C(4A)	121.43(16)
C(10A)-C(8A)	1.437(2)	C(10)-C(10A)-C(5)	122.45(16)
C(9)-C(8A)	1.397(2)	C(10)-C(10A)-C(8A)	118.74(16)
C(10)-C(4A)	1.395(2)	C(5)-C(10A)-C(8A)	118.81(16)
C(8)-C(7)	1.358(3)	C(8A)-C(9)-C(9A)	121.82(16)
C(8)-C(8A)	1.426(2)	C(4A)-C(10)-C(10A)	121.56(16)
C(7)-C(6)	1.421(3)	C(7)-C(8)-C(8A)	120.99(18)

C(5)-C(6)	1.364(3)	C(10)-C(4A)-C(4)	120.91(15)
C(14)-C(15)	1.384(3)	C(10)-C(4A)-C(9A)	119.99(15)
C(14)-C(13)	1.388(3)	C(4)-C(4A)-C(9A)	119.08(15)
C(16)-C(15)	1.390(2)	C(8)-C(7)-C(6)	120.62(17)
C(16)-C(11)	1.392(2)	C(6)-C(5)-C(10A)	120.59(17)
C(13)-C(12)	1.387(3)	C(5)-C(6)-C(7)	120.52(17)
C(12)-C(11)	1.396(2)	C(9)-C(8A)-C(8)	121.88(16)
C(17)-C(22)	1.390(2)	C(9)-C(8A)-C(10A)	119.64(15)
C(17)-C(18)	1.397(2)	C(8)-C(8A)-C(10A)	118.47(16)
C(18)-C(19)	1.384(3)	C(15)-C(14)-C(13)	120.11(17)
C(19)-C(20)	1.390(3)	C(15)-C(16)-C(11)	120.38(17)
C(20)-C(21)	1.381(3)	C(14)-C(15)-C(16)	119.86(17)
C(21)-C(22)	1.388(2)	C(12)-C(13)-C(14)	120.28(17)
		C(13)-C(12)-C(11)	119.94(17)
C(1)-P(1)-C(11)	105.61(9)	C(22)-C(17)-C(18)	119.33(16)
C(1)-P(1)-C(17)	106.41(8)	C(22)-C(17)-P(1)	119.25(13)
C(18)-C(17)-P(1)	121.39(13)	C(21)-C(22)-C(17)	120.18(17)
C(19)-C(18)-C(17)	120.22(17)	C(16)-C(11)-C(12)	119.43(16)
C(18)-C(19)-C(20)	120.01(17)	C(16)-C(11)-P(1)	120.77(13)
C(21)-C(20)-C(19)	120.02(17)	C(12)-C(11)-P(1)	119.79(13)
C(20)-C(21)-C(22)	120.22(17)		

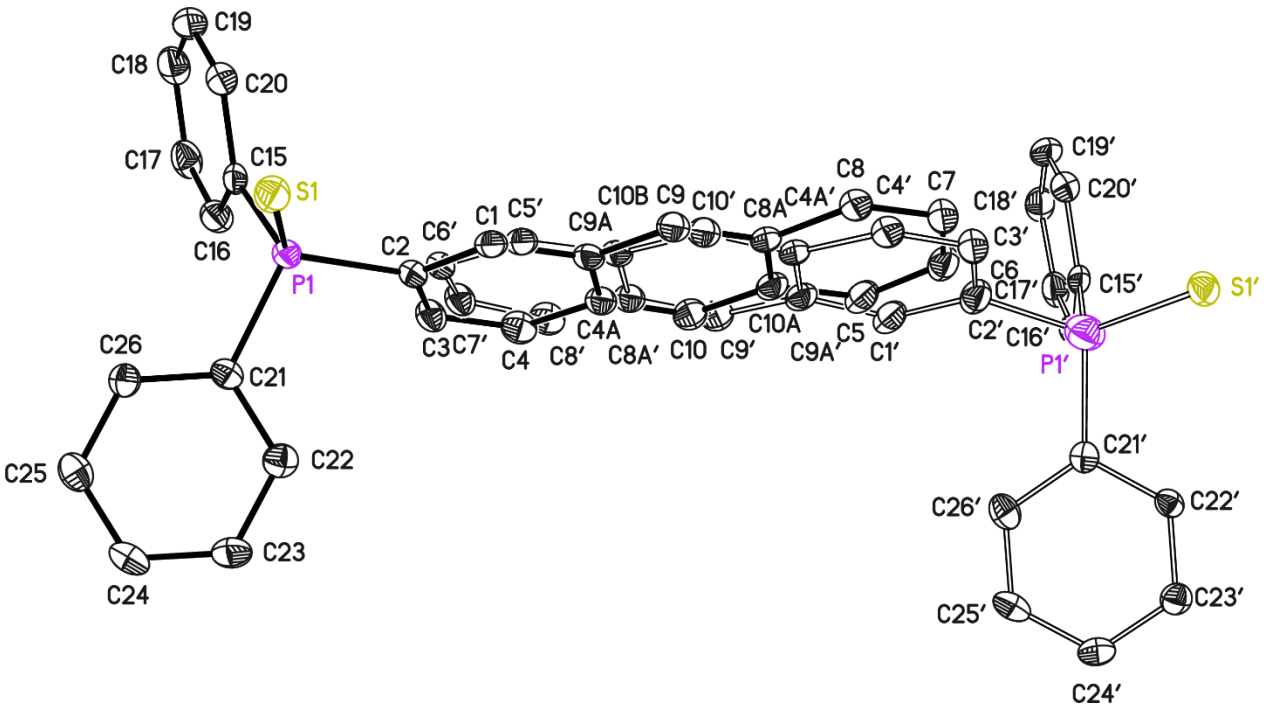

Fig. S10. Asymmetric unit of **2** with anisotropic displacement parameters at 50 % probability level. Hydrogen atoms are omitted for clarity. The molecule is disordered over two positions, whereas the substituent adopts a different orientation by rotation of around 180°. The whole structure is refined with distance restraints and restraints for the anisotropic displacement parameters.[4] The occupancy of the minor component refines to 0.0652(15).

Table S3. Bond lengths [Å] and angles [°] for **2**.			
P(1)-C(2)	1.812(2)	P(1')-S(1')	1.959(12)
P(1)-C(21)	1.816(2)	C(1')-C(2')	1.367(18)
P(1)-C(15)	1.820(2)	C(1')-C(9A')	1.402(17)
P(1)-S(1)	1.9573(9)	C(2')-C(3')	1.439(18)
C(1)-C(2)	1.367(3)	C(3')-C(4')	1.343(18)
C(1)-C(9A)	1.426(3)	C(4')-C(4A')	1.436(18)
C(2)-C(3)	1.439(3)	C(4A')-C(10')	1.365(17)
C(3)-C(4)	1.355(4)	C(4A')-C(9A')	1.449(18)
C(4)-C(4A)	1.437(3)	C(5')-C(6')	1.380(19)
C(4A)-C(10)	1.393(3)	C(5')-C(10B)	1.401(18)
C(4A)-C(9A)	1.441(3)	C(6')-C(7')	1.431(19)
C(5)-C(6)	1.366(4)	C(7')-C(8')	1.357(18)
C(5)-C(10A)	1.429(3)	C(8')-C(8A')	1.430(18)
C(6)-C(7)	1.417(4)	C(8A')-C(9')	1.368(17)
C(7)-C(8)	1.360(4)	C(8A')-C(10B)	1.453(18)

C(8)-C(8A)	1.429(3)	C(9')-C(9A')	1.394(18)
C(8A)-C(9)	1.392(3)	C(10')-C(10B)	1.401(18)
C(8A)-C(10A)	1.442(3)	C(15')-C(16')	1.390(14)
C(9)-C(9A)	1.398(3)	C(15')-C(20')	1.400(14)
C(10)-C(10A)	1.397(3)	C(16')-C(17')	1.384(15)
C(15)-C(20)	1.401(3)	C(17')-C(18')	1.374(15)
C(15)-C(16)	1.402(3)	C(18')-C(19')	1.370(15)
C(16)-C(17)	1.390(3)	C(19')-C(20')	1.382(15)
C(17)-C(18)	1.390(4)	C(21')-C(22')	1.385(14)
C(18)-C(19)	1.383(4)	C(21')-C(26')	1.391(14)
C(19)-C(20)	1.393(3)	C(22')-C(23')	1.387(15)
C(21)-C(26)	1.395(3)	C(23')-C(24')	1.373(15)
C(21)-C(22)	1.395(3)	C(24')-C(25')	1.376(15)
C(22)-C(23)	1.387(3)	C(25')-C(26')	1.386(15)
C(23)-C(24)	1.385(3)		
C(24)-C(25)	1.388(4)	C(2)-P(1)-C(21)	105.48(11)
C(25)-C(26)	1.392(3)	C(2)-P(1)-C(15)	104.94(11)
P(1')-C(2')	1.815(15)	C(21)-P(1)-C(15)	106.58(10)
P(1')-C(15')	1.823(13)	C(2)-P(1)-S(1)	113.55(9)
P(1')-C(21')	1.829(13)	C(21)-P(1)-S(1)	112.15(7)
C(15)-P(1)-S(1)	113.46(8)	C(22)-C(21)-P(1)	119.50(18)
C(2)-C(1)-C(9A)	121.4(2)	C(23)-C(22)-C(21)	120.2(2)
C(1)-C(2)-C(3)	119.5(2)	C(24)-C(23)-C(22)	120.3(2)
C(1)-C(2)-P(1)	119.66(18)	C(23)-C(24)-C(25)	120.1(2)
C(3)-C(2)-P(1)	120.85(18)	C(24)-C(25)-C(26)	119.8(2)
C(4)-C(3)-C(2)	120.7(2)	C(25)-C(26)-C(21)	120.3(2)
C(3)-C(4)-C(4A)	121.5(2)	C(2')-P(1')-C(15')	105.9(12)
C(10)-C(4A)-C(4)	122.8(2)	C(2')-P(1')-C(21')	110.3(12)
C(10)-C(4A)-C(9A)	119.5(2)	C(15')-P(1')-C(21')	105.7(11)
C(4)-C(4A)-C(9A)	117.8(2)	C(2')-P(1')-S(1')	113.1(9)
C(6)-C(5)-C(10A)	120.9(2)	C(15')-P(1')-S(1')	108.7(9)
C(5)-C(6)-C(7)	120.5(2)	C(21')-P(1')-S(1')	112.7(8)
C(8)-C(7)-C(6)	120.6(2)	C(2')-C(1')-C(9A')	125(2)
C(7)-C(8)-C(8A)	121.1(2)	C(1')-C(2')-C(3')	115.7(17)
C(9)-C(8A)-C(8)	122.3(2)	C(1')-C(2')-P(1')	122.3(16)

C(9)-C(8A)-C(10A)	119.3(2)	C(3')-C(2')-P(1')	122.0(15)
C(8)-C(8A)-C(10A)	118.4(2)	C(4')-C(3')-C(2')	122(2)
C(8A)-C(9)-C(9A)	121.8(2)	C(3')-C(4')-C(4A')	123(2)
C(9)-C(9A)-C(1)	122.1(2)	C(10')-C(4A')-C(4')	125(2)
C(9)-C(9A)-C(4A)	118.8(2)	C(10')-C(4A')-C(9A')	120.1(18)
C(1)-C(9A)-C(4A)	119.1(2)	C(4')-C(4A')-C(9A')	115.3(17)
C(4A)-C(10)-C(10A)	121.6(2)	C(6')-C(5')-C(10B)	124(2)
C(10)-C(10A)-C(5)	122.5(2)	C(5')-C(6')-C(7')	117(2)
C(10)-C(10A)-C(8A)	119.0(2)	C(8')-C(7')-C(6')	121(2)
C(5)-C(10A)-C(8A)	118.5(2)	C(7')-C(8')-C(8A')	122(2)
C(20)-C(15)-C(16)	119.6(2)	C(9')-C(8A')-C(8')	124(2)
C(20)-C(15)-P(1)	118.50(17)	C(9')-C(8A')-C(10B)	118.7(19)
C(16)-C(15)-P(1)	121.75(18)	C(8')-C(8A')-C(10B)	117.0(18)
C(17)-C(16)-C(15)	120.0(2)	C(8A')-C(9')-C(9A')	125(2)
C(18)-C(17)-C(16)	120.0(2)	C(9')-C(9A')-C(1')	125(2)
C(19)-C(18)-C(17)	120.3(2)	C(9')-C(9A')-C(4A')	115.5(18)
C(18)-C(19)-C(20)	120.4(2)	C(1')-C(9A')-C(4A')	119.0(18)
C(19)-C(20)-C(15)	119.7(2)	C(4A')-C(10')-C(10B)	124(2)
C(26)-C(21)-C(22)	119.3(2)	C(10')-C(10B)-C(5')	125(2)
C(26)-C(21)-P(1)	120.39(18)	C(10')-C(10B)-C(8A')	116.5(18)
C(5')-C(10B)-C(8A')	118.0(18)	C(22')-C(21')-C(26')	117.1(15)
C(16')-C(15')-C(20')	120.1(16)	C(22')-C(21')-P(1')	118.8(14)
C(16')-C(15')-P(1')	121.4(14)	C(26')-C(21')-P(1')	123.7(15)
C(20')-C(15')-P(1')	117.6(14)	C(21')-C(22')-C(23')	122.5(16)
C(17')-C(16')-C(15')	119.1(18)	C(24')-C(23')-C(22')	119.7(17)
C(18')-C(17')-C(16')	120.6(19)	C(23')-C(24')-C(25')	118.6(19)
C(19')-C(18')-C(17')	121(2)	C(24')-C(25')-C(26')	121.8(18)
C(18')-C(19')-C(20')	120.1(19)	C(25')-C(26')-C(21')	120.3(17)
C(19')-C(20')-C(15')	119.4(16)		

S4. Photophysical Data

Table S4. Photophysical data of **1** – **3** in diluted THF solution (10^{-5} M).				
	λ_{abs} / nm	λ_{em}[a] / nm	τ[b] / ns	Φ_F / %
1	336 / 354 / 371 / 391	378 / 402 / 424 / 450	1.1 / 5.3	< 1
2	343 / 364 / 385	401 / 423 / 448	0.9 / 8.8	< 1
3	352 / 371 / 392 / 411	462	0.1 / 9.3	< 1
[a] λ_{ex} = 350 nm; [b] λ_{ex} = 375 nm, detection at λ_{em}.				

Table S5. Photophysical data of **1** – **3** in the solid-state.			
	λ_{em}[a] / nm	τ[b] / ns	Φ_F / %
1	545	29.0	5.9
2	426 / 441 / 469 / 502	3.2 / 7.8	15.7
3	484	1.4 / 3.2	4.0
[a] λ_{ex} = 375 nm; [b] λ_{ex} = 375 nm, detection at λ_{em}.			

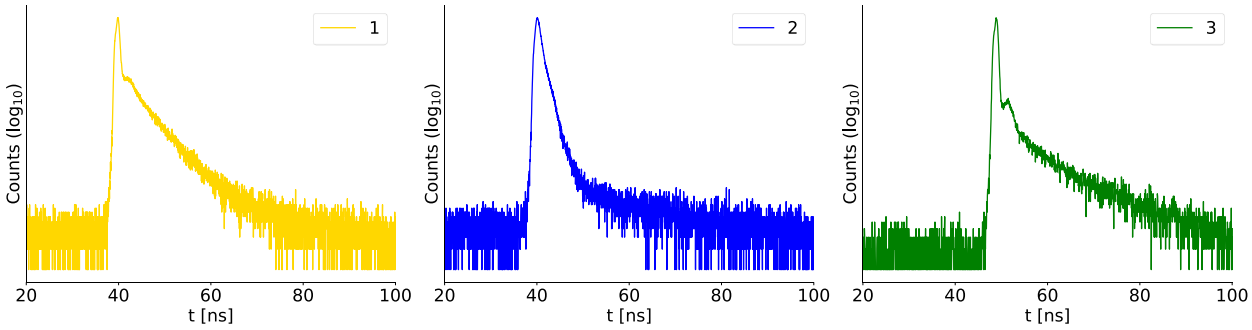

Fig. S11. Fluorescence lifetime decay plots of **1** (left), **2** (middle) and **3** (right) in diluted THF solution (10-5 M, λ_{ex} = 375 nm). Lifetimes were fitted as one or two-dimensional decays.

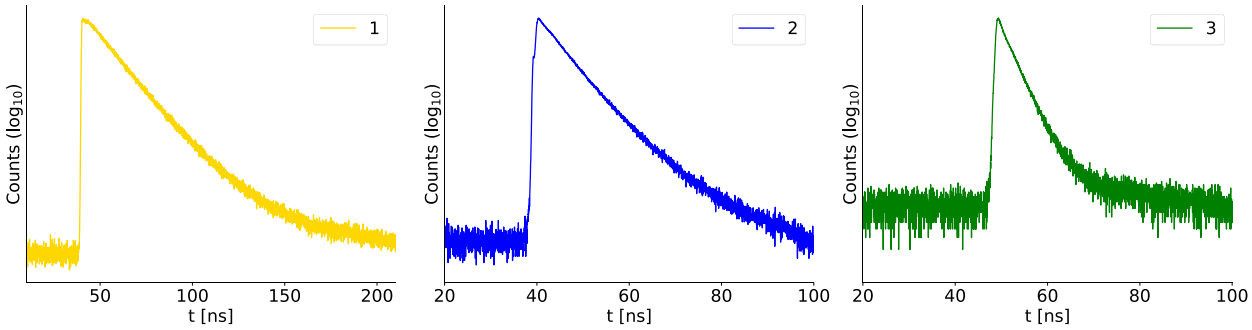

Fig. S12. Fluorescence lifetime decay plots of **1** (left), **2** (middle) and **3** (right) in the solid-state (λ_{ex} = 375 nm). Lifetimes were fitted as one or two-dimensional decays.

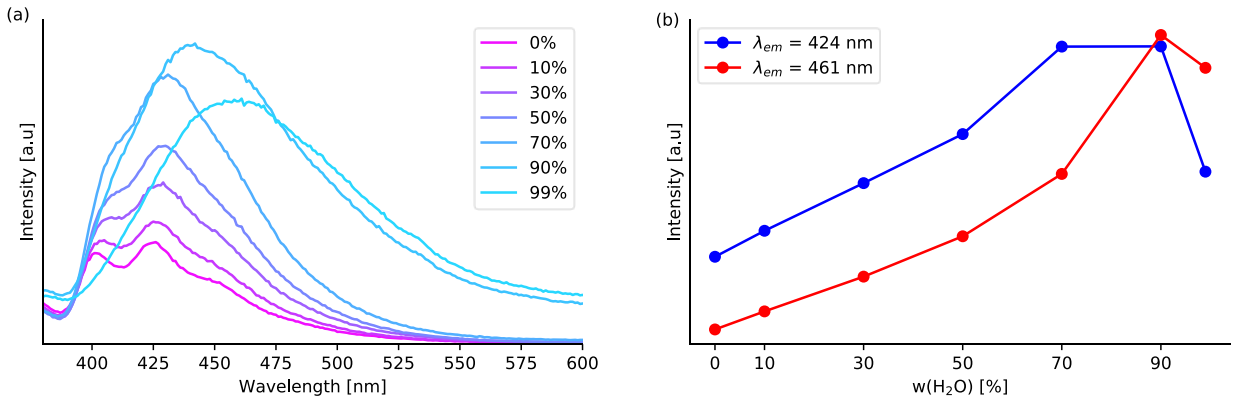

Fig. S13. (a) Emission spectra of **1** in THF/H_2O mixtures (10^{-5} M) with different H_2O fractions w. (b) Observed emission intensity at the emission wavelengths 424 nm (blue) and 461 nm (red).

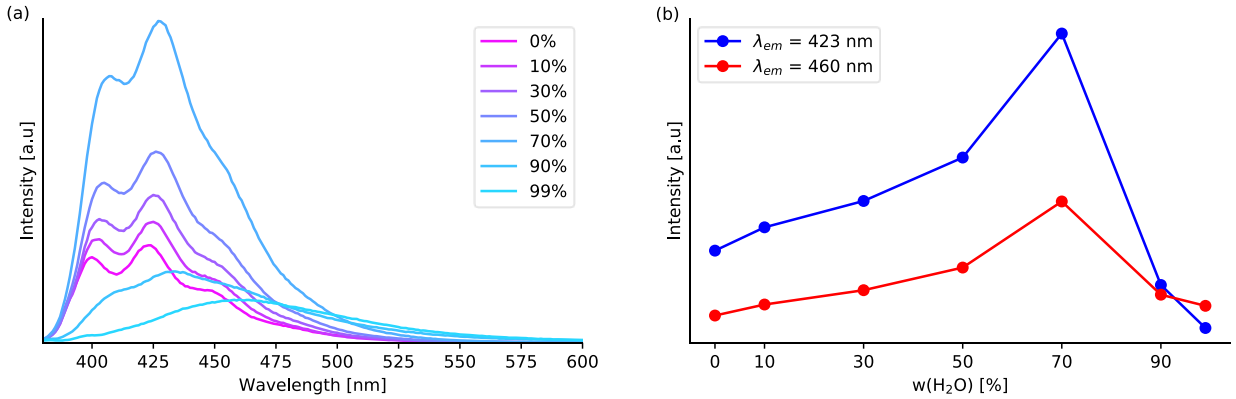

Fig. S14. (a) Emission spectra of **2** in THF/H_2O mixtures (10^{-5} M) with different H_2O fractions w. (b) Observed emission intensity at the emission wavelengths 423 nm (blue) and 460 nm (red).

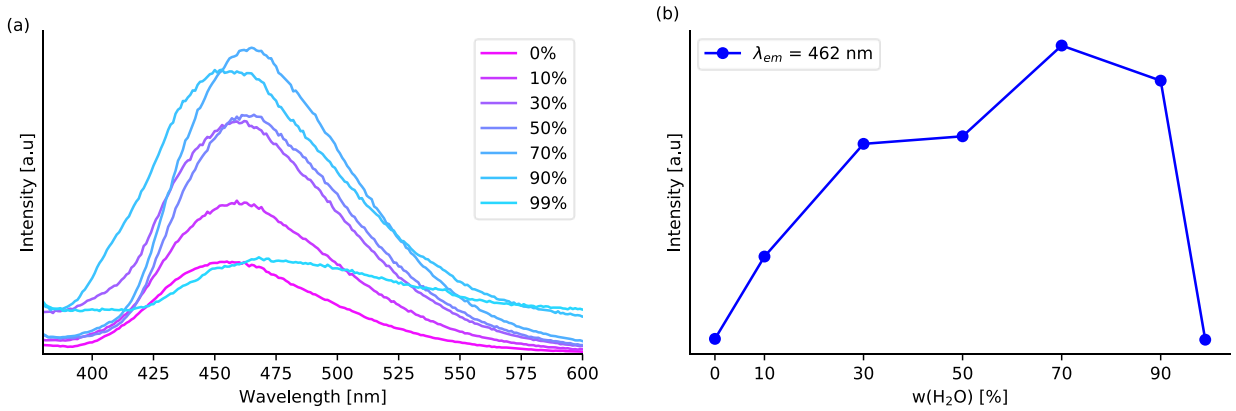

Fig. S15. (a) Emission spectra of **3** in THF/H_2O mixtures (10^{-5} M) with different H_2O fractions w. (b) Observed emission intensity at the emission wavelengths 462 nm.

S5. NMR Spectroscopic data

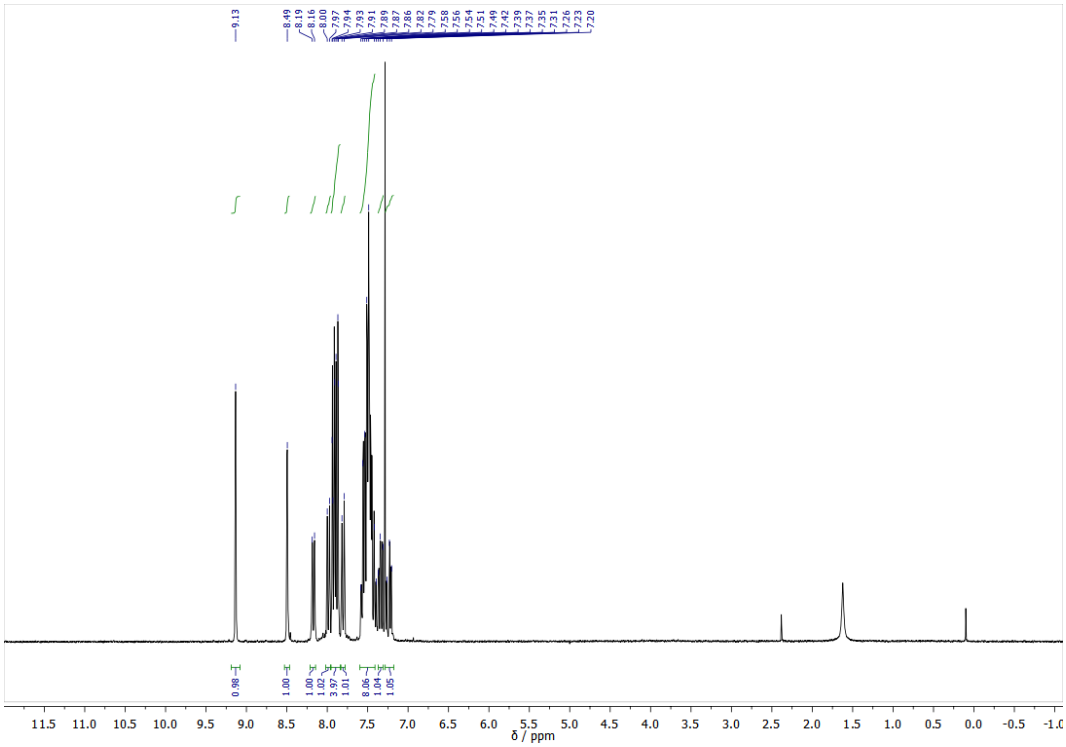

Fig. S16. ^{1}H-NMR of [1-(S)PPh$_2$(C$_{14}$H$_9$)] (**1**) in CDCl$_3$.

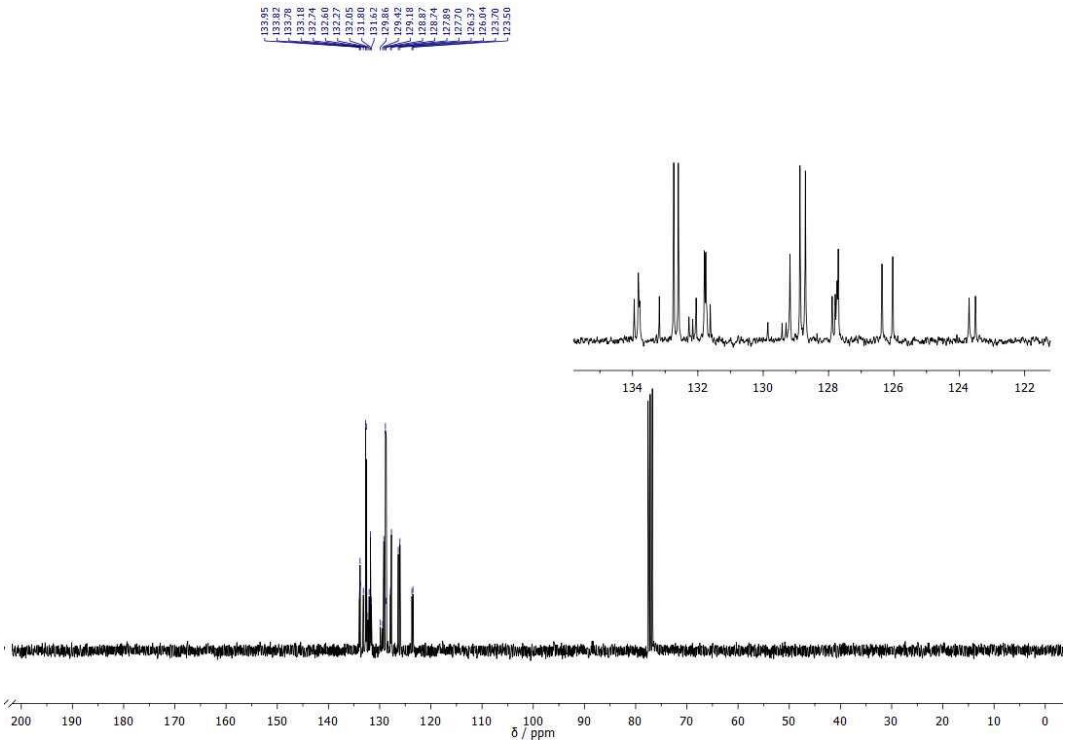

Fig. S17. ^{13}C{^{1}H}-NMR of [1-(S)PPh$_2$(C$_{14}$H$_9$)] (**1**) in CDCl$_3$.

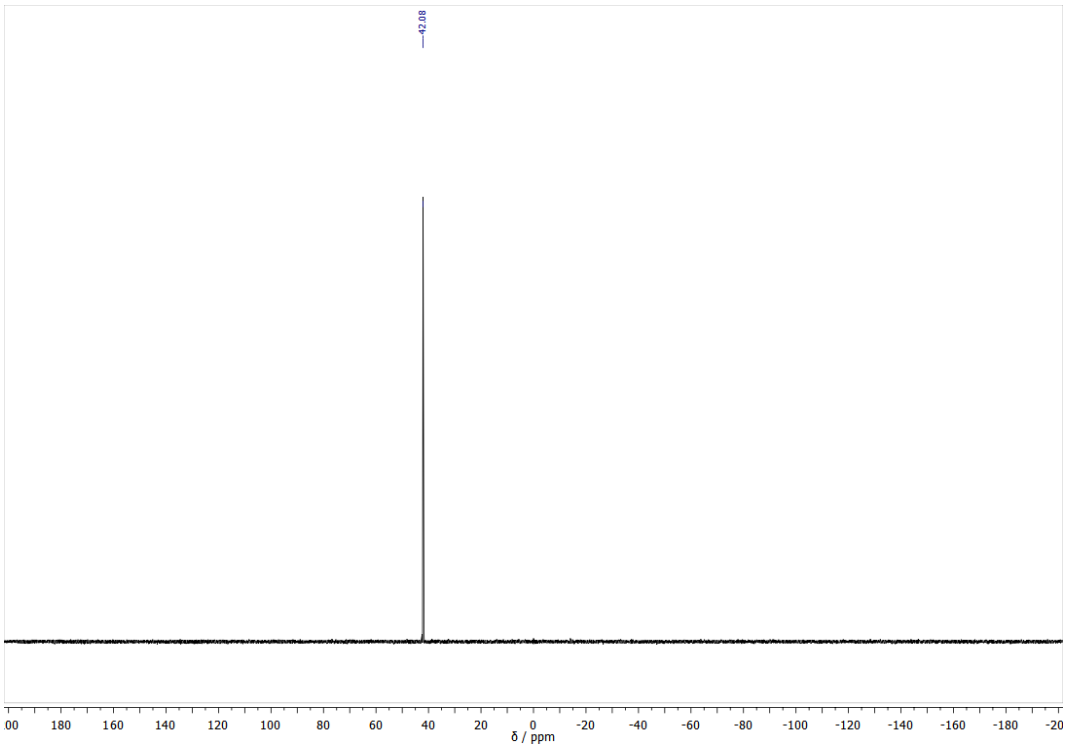

Fig. S18 $^{31}P\{^{1}H\}$-NMR of [1-(S)$PPh_2(C_{14}H_9)$] (**1**) in $CDCl_3$.

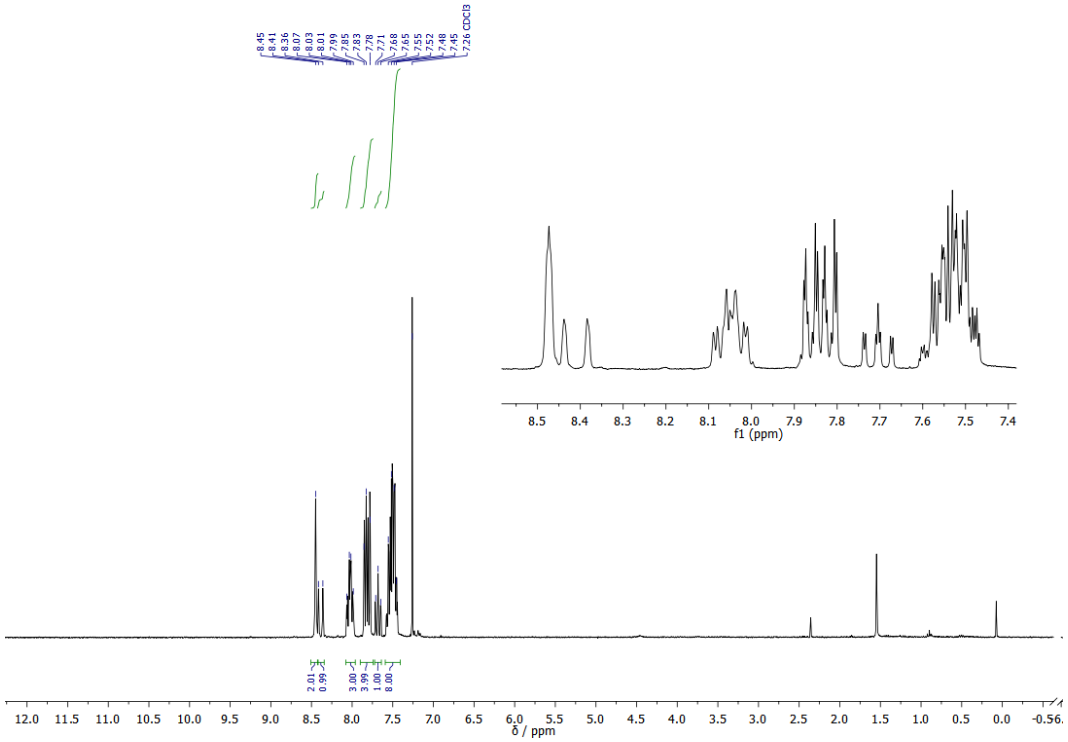

Fig. S19. ^{1}H-NMR of [2-(S)$PPh_2(C_{14}H_9)$] (**2**) in $CDCl_3$.

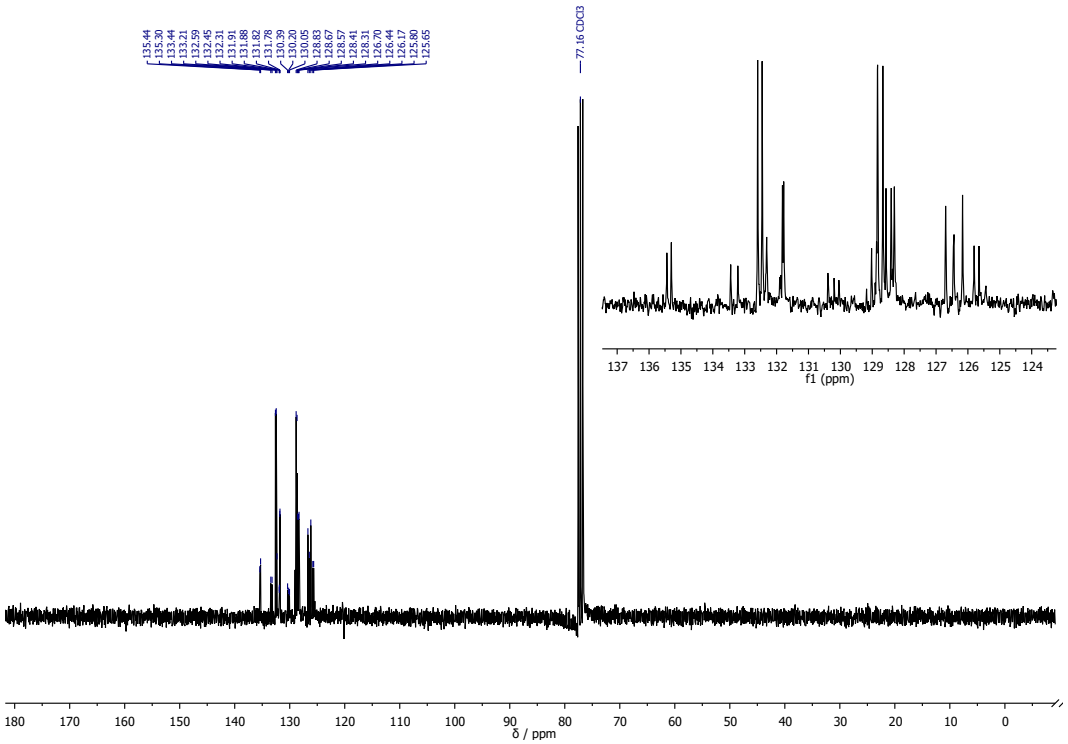

Fig. S20. $^{13}C\{^{1}H\}$-NMR of [2-(S)$PPh_2(C_{14}H_9)$] (**2**) in $CDCl_3$.

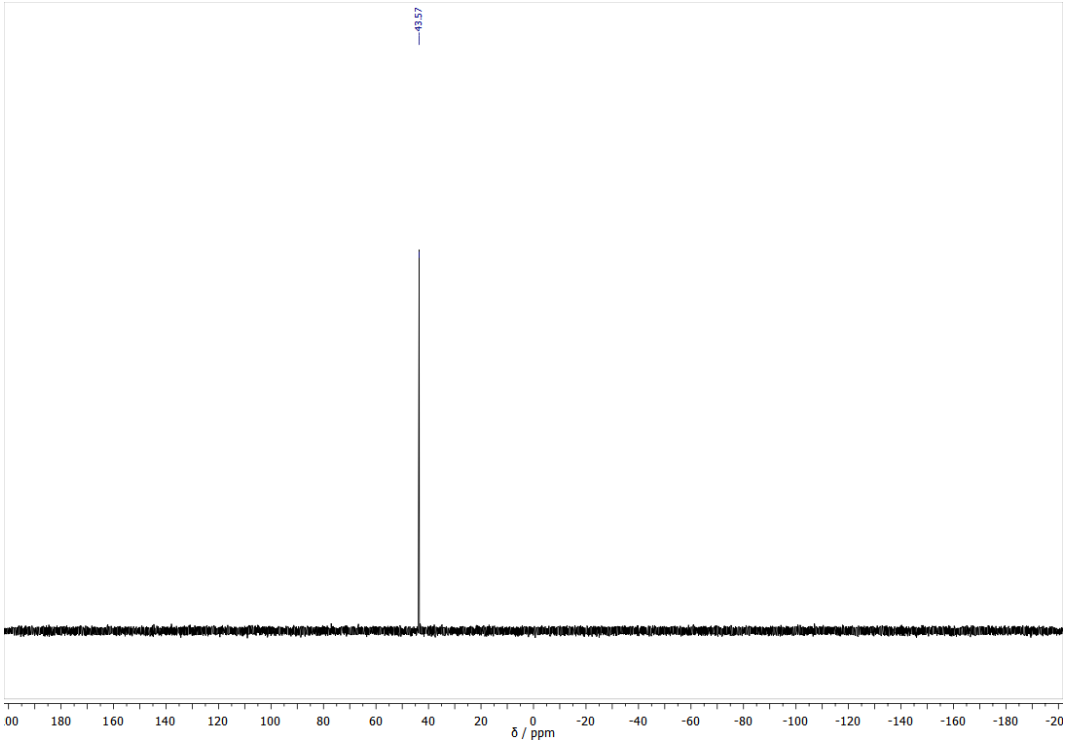

Fig. S21. $^{31}P\{^{1}H\}$-NMR of [2-(S)$PPh_2(C_{14}H_9)$] (**2**) in $CDCl_3$.

S6. References

[1] Virtuelles Labor I, http://www.stalke.chemie.uni-goettingen.de/virtuelles_labor/advanced/13_de.html, (accessed 1st January 2020).

[2] J. Moursounidis and D. Wege, *Austr. J. Chem.*, 1988, **41**, 235.

[3] K. Ito, T. Suzuki, Y. Sakamoto, D. Kubota, Y. Inoue, F. Sato and S. Tokito, *Angew. Chem., Int. Ed.*, 2003, **42**, 1159.

[4] A. Thorn, B. Dittrich, G. M. Sheldrick, Acta Crystallogr. **2012**, *A68*, 448.